

# Probabilistic Data Association for Tracking Extended Targets Under Clutter Using Random Matrices

Michael Schuster, Johannes Reuter  
Institute of System Dynamics  
Konstanz University of Applied Sciences  
michael.schuster,johannes.reuter@htwg-konstanz.de

Gerd Wanielik  
Professorship of Communication Engineering  
Chemnitz University of Technology  
gerd.wanielik@etit.tu-chemnitz.de

**Abstract**—The use of random matrices for tracking extended objects has received high attention in recent years. It is an efficient approach for tracking objects that give rise to more than one measurement per time step. In this paper, the concept of random matrices is used to track surface vessels using high-resolution automotive radar sensors. Since the radar also receives a large number of clutter measurements from the water, for the data association problem, a generalized probabilistic data association filter is applied. Additionally, a modification of the filter update step is proposed to incorporate the Doppler velocity measurements. The presented tracking algorithm is validated using Monte Carlo Simulation, and some performance results with real radar data are shown as well.

## I. INTRODUCTION

Radar systems have become standard for vessel detection and collision avoidance in marine navigation. Owing to the required high angular resolution, typical radars for inland waterways have large apertures and high power consumptions. As recreational crafts or small unmanned surface vessels do not usually have sufficient space for such systems, automotive radar sensors are an interesting alternative. Working at a higher frequency, these sensors offer comparable angular resolutions and accurate Doppler velocity measurements at the price of a reduced detection range and scanning angle. However, due to the extension of a vessel in comparison with sensor resolution, at each scan, the sensor provides several detections of an object. This leads to an extended target tracking problem according to the definition of an extended target in [1]. The problem of tracking extended targets has been the subject of research for many years, which is why a large variety of algorithms have already been proposed. Surveys on this topic can be found in [2] and [3]. Considering a sensor that receives a point cloud from the illuminated object, new sensor models have been developed that can roughly be divided into two different core assumptions:

One model group assumes that the sources of the measurements are at distinct locations within the target and, in some cases, can be used to reconstruct the target's shape. A model for the simulation of the received measurement from a vehicle using automotive radar sensor was introduced by [4]. This model is based on the assumption that a vehicle

consists of a set of point reflection centers and plane reflectors. On the basis of this sensor model, a tracking framework was presented by [5]. However, the exact prediction of the location of the reflection centers requires detailed knowledge of the target type under observation. If no prior information about the location of reflection centers is available, the concept of tracking individual measurement generating points of an object was also used in [6],[7].

However, in many applications, not stable but fast fluctuating reflection centers are the case. Hence, alternative sensor models assume that the measurements are randomly distributed over the target extent during the observation process. Further, it is assumed that the noise of the measurements is correlated with the size of the target. Thus, by analyzing the noise distribution, an estimation of the target extent can be obtained. An approach when the shape of the target is elliptical is presented in [8]. The target's physical extension is represented by a random symmetric positive definite matrix. An alternative to arbitrary shapes is presented in [9], where Random Hypersurface Models are used to estimate the extent of an object. In case the measurement spread is only partially depended on the target extent and also on the sensor accuracy, [10] proposed modeling this spread as a linear combination of extension noise and measurement noise. Using the heuristics in [10], [11] derived a more complex filter update step that improves the estimation results. A unification of [8] and [10] was proposed in [12], and further extended for non-elliptical models in [13].

All referenced papers on Random Matrices so far assume that the data association problem is solved. Nevertheless, only a few algorithms that deal with the data association problem have been presented. In [14] and [15], the PMHT is applied to solve the data association problem. Using a spatial clustering of the detections in combination with an JPDA is proposed in [16] and a PHD-based approach is presented in [17].

As an alternative, the Generalized Probabilistic Data Association (GPDA) filter is considered here. For each detection within a gate, the well-known PDA calculates a probability for the hypothesis that it was generated by the target [18]. Therefore, the assumption is made that at the most the target

originates one detection. [19] proposed an extension to the PDA. Termed Multiple Detection Probabilistic Data Association, here the association likelihoods were calculated under the condition that more than one measurement was created by the target. Comparable to the IPDA, the filter was then extended in [20] to incorporate the existence likelihood and was applied in [21] for extension estimation. The GPDA is then used to estimate the width of a vehicle. If each transmitted radar spoke within a scan has equal likelihood to evoke a measurement from the extended target, the cardinality of measurements is binomially distributed. Similar to the PDA, the multiple detection JPDA is presented in [22]. The MD-JPDA was used to handle multi-path reflections from over-the-horizon radars.

In this paper, the G(J)PDA is applied to track one or more vessels under clutter, and to estimate kinematic state and physical extent using the concept of random matrices. Therefore, the paper is structured as follows: Section II gives a brief overview of Random Matrices while a modification to incorporate Doppler measurement is proposed in Section III. Section IV describes the GPDA filter and in Section V some considerations regarding the implementation and some simulation results are presented. Finally, the results for a real target tracking scenario are presented, followed by a short conclusion.

## II. RANDOM MATRICES

The seminal work applying random matrices for estimation of extended objects was presented in [8]. In this work, a concept to obtain an estimate of the kinematic target state and its physical extension using Bayes' theorem was established. Therefore, a few assumptions on the target characteristics are made. First, it is assumed that the shape of the target can be represented by an ellipse. Further, it is assumed that there is no correlation between the orientation of the ellipse and the direction of the object's motion. This is required for vessel tracking since during maneuvers, or when a vessel is just drifting with the sea current (e.g. fishermen), no alignment of principal axis to the direction of motion is given.

The most important assumption required for the use of random matrices affects the measurement noise: The noise is mainly caused by the physical extension. Given a measurement  $\mathbf{z}_k^j$  at time  $k$ , a linear relationship to a state  $\mathbf{x}_k$  is assumed, which is superimposed by a normally distributed noise term  $\mathbf{w}_k$ :

$$\mathbf{z}_k^j = \mathbf{H}\mathbf{x}_k + \mathbf{w}_k \quad (1)$$

The physical extension of the object at time  $k$  is described by a symmetric positive definite random matrix  $\mathbf{X}_k$ . Assuming that the noise part of the measurement is mainly due to the size of the object, the probability density function for a set of measurements  $\mathbf{Z}_k = \left\{ \mathbf{z}_k^j \right\}_{j=1}^{n_k}$  is defined as:

$$p(\mathbf{Z}_k | n_k, \mathbf{x}_k, \mathbf{X}_k) = \prod_{j=1}^{n_k} \mathcal{N}(\mathbf{z}_k^j; \mathbf{H}\mathbf{x}_k, \mathbf{X}_k) \quad (2)$$

By calculating the center of gravity for the measurement set

$$\bar{\mathbf{z}}_k = \frac{1}{n_k} \sum_{j=1}^{n_k} \mathbf{z}_k^j \quad (3)$$

and the outer product of the measurements

$$\bar{\mathbf{Z}}_k = \sum_{j=1}^{n_k} (\mathbf{z}_k^j - \bar{\mathbf{z}}_k)(\mathbf{z}_k^j - \bar{\mathbf{z}}_k)^T \quad (4)$$

the pdf in (2) can be rewritten in the form

$$p(\mathbf{Z}_k | n_k, \mathbf{x}_k, \mathbf{X}_k) \propto \mathcal{N}(\bar{\mathbf{z}}_k; \mathbf{H}\mathbf{x}_k, \mathbf{X}_k / n_k) \times \mathcal{W}(\bar{\mathbf{Z}}_k; n_k - 1, \mathbf{X}_k), \quad (5)$$

where  $\mathcal{W}$  denotes a Wishart distribution over  $\mathbf{X}_k$  with  $n_k - 1$  degrees of freedom. Substituting this relationship in the Bayes' filter recursion leads to an analytic solution for state expectation and covariance update as well as for the update of  $\mathbf{X}_k$ .

However, radar detections are generally in polar coordinates with range  $r$  and detection angle  $\phi$ . Thus, if targets are detected in greater distance, this leads to a larger spread of the measurements. Disregarding this fact for the estimation of the physical extension would lead to an overestimation of the true size when the object is far away.

To include the contribution of the sensor error to the measurement spread, [10] proposed rewriting the probability density function in the following way:

$$p(\mathbf{Z}_k | n_k, \mathbf{x}_k, \mathbf{X}_k) = \prod_{j=1}^{n_k} \mathcal{N}(\mathbf{z}_k^j; \mathbf{H}\mathbf{x}_k, c\mathbf{X}_k + \mathbf{R}_k) \quad (6)$$

However, for this model, no exact analytical solution can be found for  $p(\mathbf{x}_k, \mathbf{X}_k | \mathbf{Z}^k)$ . To obtain a recursive update scheme, in [10] the assumption is made that the target extent is predicted with sufficient accuracy, which makes it possible to separate kinematic and extension updates. With some further approximations, the following filter scheme is obtained:

Kinematic:	
$\mathbf{x}_{k k}$	$= \mathbf{x}_{k k-1} + \mathbf{K}_{k k-1}(\bar{\mathbf{z}}_k - \mathbf{H}\mathbf{x}_{k k-1})$
$\mathbf{P}_{k k}$	$= \mathbf{P}_{k k-1} + \mathbf{K}_{k k-1}\mathbf{H}\mathbf{P}_{k k-1}^T$
$\mathbf{S}_{k k-1}$	$= \mathbf{H}\mathbf{P}_{k k-1}\mathbf{H}^T + \frac{1}{n_k}\mathbf{Y}_{k k-1}$
$\mathbf{K}_{k k-1}$	$= \mathbf{P}_{k k-1}\mathbf{H}^T\mathbf{S}_{k k-1}^{-1}$
$\mathbf{Y}_{k k-1}$	$= c\mathbf{X}_{k-1 k-1} + \mathbf{R}_k$
Extension:	
$\mathbf{X}_{k k}$	$= \frac{1}{\alpha_k}(\alpha_{k k-1}\mathbf{X}_{k k-1} + \hat{\mathbf{N}}_{k k-1} + \hat{\mathbf{Y}}_{k k-1})$
$\alpha_k$	$= \alpha_{k k-1} + n_k$
$\mathbf{N}_{k k-1}$	$= (\bar{\mathbf{z}}_k - \mathbf{H}\mathbf{x}_{k k-1})(\bar{\mathbf{z}}_k - \mathbf{H}\mathbf{x}_{k k-1})^T$
$\hat{\mathbf{N}}_{k k-1}$	$= \mathbf{X}_{k k-1}^{1/2}\mathbf{S}_{k k-1}^{-1/2}\mathbf{N}_{k k-1}^{1/2}(\mathbf{S}_{k k-1}^{-1/2})^T(\mathbf{X}_{k k-1}^{-1/2})^T$
$\hat{\mathbf{Y}}_{k k-1}$	$= \mathbf{X}_{k k-1}^{1/2}\mathbf{Y}_{k k-1}^{-1/2}\bar{\mathbf{Z}}_{k k-1}^{1/2}(\mathbf{Y}_{k k-1}^{-1/2})^T(\mathbf{X}_{k k-1}^{-1/2})^T$

TABLE I  
FILTER UPDATE STEPS [10]

The prediction step for the kinematic state is the same as for the well-known Kalman filter. For the extension, a time

$\tau$  is applied in order to describe the time-restricted change in the extension. Using  $T$  for the sample time, the predictions are shown in Table II.

Kinematic:	
$\mathbf{x}_{k k-1}$	$= \mathbf{F}_k \mathbf{x}_{k-1 k-1}$
$\mathbf{P}_{k k-1}$	$= \mathbf{F}_k \mathbf{P}_{k-1 k-1} \mathbf{F}_k^T + \mathbf{Q}_k$
Extension:	
$\alpha_{k k-1}$	$= 2 + e^{-\frac{T}{\tau}} (\alpha_{k-1 k-1} - 2)$
$\mathbf{X}_{k k-1}$	$= \mathbf{X}_{k-1 k-1}$

TABLE II  
FILTER PREDICTION STEPS [10]

As already mentioned in the introduction, a more general update scheme using the sensor model as in (6) was presented in [11]. However, the focus of this paper is on data association for RM. The improvements of [11] are not further discussed here, since those lead to a significantly more complex filter scheme. Nevertheless, based on the approach of [10], in the next section, an extension to incorporate range rate measurements in the measurement update step is considered.

### III. EXTENSION FOR DOPPLER MEASUREMENTS

Especially when radar sensors are used, in addition to the polar position measurements, the Doppler velocity or range rate is available. In general, the range rate is a valuable piece of information that can significantly improve the kinematic state estimate, especially when a target is performing fast maneuvers. Thus, the range rate should be used in the track filtering process as well. However, no direct transformation of the range rate into the Cartesian space is possible, so an alternative representation of the measurement model is proposed: Assuming that the sensor provides the typical radar measurements range  $r$ , bearing  $\phi$  and range rate  $\dot{r}$ , the measurement model is given by

$$\mathbf{z}_k = \mathbf{h} \left( \begin{array}{c} \sqrt{x^2 + y^2} \\ \tan^{-1} y/x \\ \frac{xv_x + yv_y}{\sqrt{x^2 + y^2}} \end{array} \right) + \mathbf{w}_k, \quad (7)$$

where  $x, y$  are the target coordinates relative to the radar, the relative target velocity  $v_x, v_y$ , and measurement noise  $\mathbf{w}_k$ . Based on the concept presented in [12], the following is proposed: Assuming the extension of the ellipse is described in a two-dimensional Cartesian space, the probability density of  $\mathbf{w}_k$  for  $n_k$  measurements is defined as

$$p(\mathbf{Z}_k | n_k, \mathbf{x}_k, \mathbf{X}_k) = \prod_{j=1}^{n_k} \mathcal{N}(\mathbf{z}_k^j; \mathbf{h}(\mathbf{x}_k), c\mathbf{B}_k \mathbf{X}_k \mathbf{B}_k^T + \mathbf{R}_k). \quad (8)$$

Under the assumption that the current target state is sufficient accurately known, the Jacobian matrix  $\mathbf{B}_k$  is given by

$$\mathbf{B}_k = \begin{bmatrix} \frac{x}{\sqrt{x^2 + y^2}} & \frac{y}{\sqrt{x^2 + y^2}} \\ -\frac{y}{x^2 + y^2} & \frac{x}{x^2 + y^2} \\ \frac{y(v_x y - v_y x)}{\sqrt{(x^2 + y^2)^3}} & \frac{x(v_y x - v_x y)}{\sqrt{(x^2 + y^2)^3}} \end{bmatrix} \quad (9)$$

and  $\mathbf{R}_k$  is now the measurement noise covariance matrix in polar coordinates. However,  $\mathbf{B}_k$  only valid if the differential Doppler speed due to the object turn rate is small. Since there is a nonlinear relationship between state and measurement, here the Unscented Transform [23] is proposed to update the kinematic state estimate. The update of the extension estimate can be obtained in a straightforward manner by replacing  $\mathbf{X}_k$  with  $\mathbf{B}_k \mathbf{X}_k \mathbf{B}_k^T$  in Table I. Alternatively, it can be done by first transforming the measurements and the noise covariance  $\mathbf{Y}_{k|k-1}$  into Cartesian coordinates using the corresponding Jacobi matrix.

In [8] and [10], the acceleration model by van Keuk was used for the target's kinematic state prediction. It allows statistically independent movements in  $x$  and  $y$ -direction. However, when the detection count is a small single-digit value, the prediction step becomes more important, and the use of correlations between  $x$  and  $y$  motion, e.g. a turn rate, might improve the state estimate. It was already shown in [24] that using a horizontal turn model improves the estimate of the target's heading, which for a collision avoidance system is as important as the target's position. Knowledge about the target's turn rate can also improve the extension estimation as carried out in [25]. Thus, in this work, the constant turn rate and velocity (CTRV) model with  $\mathbf{x}_k = [x, y, \psi, \omega, V]$  is considered, where  $\psi_k$  and  $\omega$  are respectively the heading and the corresponding turning rate, and  $V_k$  the horizontal velocity. See [26] for further details.

### IV. PROBABILISTIC DATA ASSOCIATION FOR MULTIPLE DETECTIONS

The Generalized Probabilistic Data Association Filter relaxes the assumption of the PDA filter that an object can generate at the most one measurement at time  $k$ . For the GPDA, it will be assumed that up to  $n_k$  measurements can be originated by an object.

#### A. Single Object Tracking

To begin with, the case that only one object is present will be considered. In [20], the posterior probability density function is defined as a weighted sum over all association hypotheses. Let  $\mathbf{Z}^k$  denote the sets of measurements received up to time  $k$ , hence the posterior for kinematic state  $\mathbf{x}_k$  and extension  $\mathbf{X}_k$  at time  $k$  is given by

$$p(\mathbf{x}_k, \mathbf{X}_k | \mathbf{Z}^k) = \sum_{A_i^m \in A} p(\mathbf{x}_k, \mathbf{X}_k | \mathbf{Z}^k, A_i^m) P(A_i^m | \mathbf{Z}^k). \quad (10)$$

Here the hypothesis set  $A$  contains all possible associations, where  $A_i^m$  describes the  $i$ th combination of assigning  $m = 0..n_k$  measurements to the track and  $n_k$  the total number of measurements received at time  $k$ . For example, if  $n_k = 3$  there are three different combinations of assigning  $m = 2$  measurements:  $A_1^2 : \mathbf{z}_k^{(1)}, \mathbf{z}_k^{(2)}$ ,  $A_2^2 : \mathbf{z}_k^{(1)}, \mathbf{z}_k^{(3)}$  and  $A_3^2 : \mathbf{z}_k^{(2)}, \mathbf{z}_k^{(3)}$ .

The term  $p(\mathbf{x}_k, \mathbf{X}_k | \mathbf{Z}^k, A_i^m)$  can then be computed, e.g. using the filter operations as presented in Section II. For

the association probability  $P(A_i^m|\mathbf{Z}^k)$ , invoking Bayes' rule yields

$$P(A_i^m|\mathbf{Z}^k) = \frac{1}{\eta} p(\mathbf{Z}_k|A_i^m, \mathbf{Z}^{k-1}) p(A_i^m|\mathbf{Z}^{k-1}) \quad (11)$$

with the normalization factor

$$\eta = p(\mathbf{Z}_k|\mathbf{Z}^{k-1}) = \sum_{A_i^m \in A} p(\mathbf{Z}_k|A_i^m, \mathbf{Z}^{k-1}). \quad (12)$$

Assuming that the association likelihood is only dependent on the measurements at time  $k$  and making the reasonable assumption that the prior probability  $P(A_i^m)$  is uniformly distributed, the last term in (11) can be safely removed.

Next, the measurement set can be divided into a part  $\mathbf{Z}_{k,x}$ , which contains measurements that were generated by the objects and a part  $\mathbf{Z}_{k,cl}$  that contains false alarms:

$$p(\mathbf{Z}_k|A_i^m, \mathbf{Z}^{k-1}) = p(\mathbf{Z}_{k,x}|A_i^m, \mathbf{Z}^{k-1}) p(\mathbf{Z}_{k,cl}|A_i^m). \quad (13)$$

Here the additional clutter is assumed to be independent of  $\mathbf{Z}^{k-1}$ . Each part in (13) is now further separated into a spatial and a cardinality likelihood. Therefore, no correlations between target motion and target size is considered, that means each likelihood is independent.

According to the sensor model (6), the measurements are normally distributed over object extension and measurement noise. Thus, the spatial likelihood is given as product over all assigned measurements  $j$  in Hypothesis  $A_i^m$ :

$$p(\{\mathbf{z}\}_k^x|A_i^m, \mathbf{Z}^{k-1}) = \prod_{\mathbf{z}_k^j \in A_i^m} \mathcal{N}(\mathbf{z}_k^j; \mathbf{H}\mathbf{x}_k, c\mathbf{X}_k + \mathbf{R}_k) \quad (14)$$

Alternatively, the sensor model in (2) or (8) can be used.

For the sake of simplicity, the cardinality likelihood of the true measurements is proposed to be  $P(n_x|\mathbf{Z}^{k-1}, A_i^m) = P(n_x)$ . This is in accordance with the assumption in [8] that the number of measurements is independent of the target extent. However, since for real sensors this will not be the case, far more modeling effort should be made here. The most common assumption used for extended targets is that  $P(n_x)$  satisfies a Poisson distribution.

For clutter measurements, the commonly used assumption that they are uniformly distributed over the surveillance volume  $V$  with density  $\lambda$  is applied and the number of false alarms is assumed to be Poisson distributed:

$$p(\{\mathbf{z}\}_k^{cl}|A_i^m) = V^{-(n_k-m)} \quad (15)$$

$$P(n_{cl} = n_k - m|A_i^m) = \frac{(\lambda V)^{n_k-m}}{(n_k - m)!} e^{-\lambda V} \quad (16)$$

These likelihoods follow from the fact that all measurements not assigned to an object are clutter measurements. Hence, for each association hypothesis, the definition  $n_x + n_{cl} = n_k$  must hold.

With these considerations, the probability  $P(A_i^m|\mathbf{Z}^k)$  can be calculated with

$$P(A_i^m|\mathbf{Z}^k) = \frac{1}{\eta} P(n_x = m) \frac{n_k! \lambda^{-m}}{(n_z - m)!} \prod_{\mathbf{z}_k^j \in A_i^m} \mathcal{N}(\mathbf{z}_k^j; \mathbf{H}\mathbf{x}_k, c\mathbf{X}_k + \mathbf{R}_k). \quad (17)$$

After executing the update step, e. g. according to table I for each combination, the resulting estimates are merged using the determined association likelihood and a first- and second-order moment matching as presented in [10].

## B. Multi Object Tracking

The obtained GPDA filter can only be applied for multi-object cases if the objects are well separated in the measurement space. If the targets are close together, the GPDA will tend to merge tracks. To avoid this, the GJPDA can be used to consider joint track to measurement associations. Similar to the JPDA, this requires extending the set of hypotheses  $A$  for all possible combinations that distribute up to  $n_k$  measurements to  $n_T$  tracks. Let  $A_i^M = \{A_i^{m_1}, \dots, A_i^{m_{n_T}}\}$  denote the  $i$ th hypothesis to associate  $m_1$  detections to track 1 up to  $m_{n_T}$  detections to track  $n_T$ . Using the same assumptions for spatial and cardinality distribution as for the GPDA, the unnormalized association likelihood is provided by

$$P(A_i^M|\mathbf{Z}^k) = \frac{n_k! \lambda^{-m_T}}{(n_k - m_T)!} \quad (18)$$

$$\times \prod_{A_i^{m_t} \in A_i^M} P(n_x = m_t) \prod_{\mathbf{z}_k^j \in A_i^{m_t}} \mathcal{N}(\mathbf{z}_k^j; \mathbf{H}\mathbf{x}_k^{(t)}, c\mathbf{X}_k^{(t)} + \mathbf{R}_k)$$

where  $m_T = m_1 + \dots + m_{n_T} \leq n_k$  is the number of all assigned detections in this hypothesis and  $\mathbf{x}_k^{(t)}, \mathbf{X}_k^{(t)}$  denote kinematic state and extension of the  $t$ th track. The hypothesis set  $A$  in general now contains several hypotheses that assign the same measurement combinations for the  $n_j$ th track. Thus, after normalizing (18) for each track, the association weights of its  $l$ th measurement combination are marginalized over all  $A_i^M$  that contain this combination.

## V. IMPLEMENTATION

First, the algorithms have been evaluated using simulated data. In the simulations, one or two objects with the typical size of a recreational craft are moving on meander-like trajectories. It is also assumed that the major axis of the extension ellipse is aligned with the direction of motion of the target. In general, this is not true for real ships, especially because during turning maneuvers ships have significant drift angles. However, since in the modeling process the independence of extension and motion is granted, this assumption can be made to simulate the change in orientation of the ellipse during the turning maneuvers.

The object is observed by a high-resolution sensor with noise term according to Table III. The scan rate for the sensor is  $f_s = 1/T = 15Hz$ . The measurements are assumed to be uniformly distributed over the complete vessel extension. The number of received measurements from the object is Poisson-distributed with mean  $n_x = 4$ , hence the cardinality likelihood for detections from the target is given by

$$P(n_x = m|A_i^m) = \frac{(n_x)^m}{m!} e^{-n_x}. \quad (19)$$

Clutter measurements are assumed to be uniformly distributed over the complete observation space. Their number is also

Poisson with mean  $N_{cl} = 20$ , and for simplicity, the observation space is rectangular with a size of  $250m \times 250m$ .

Range	Bearing	Range Rate
$\sigma_r=0.25m$	$\sigma_\phi=1^\circ$	$\sigma_r=0.1m/s$

TABLE III  
MEASUREMENT NOISE PARAMETERS FOR POINT TARGET

Two different filter schemes, Filters A and B, were evaluated. For Filter A, a linear system of the form

$$\mathbf{x}_F = \mathbf{F}\mathbf{x}_{k-1} + \mathbf{w}_k \quad (20)$$

is considered, where only the position measurements are taken into account according to (1). In the simulation, all measurements are generated in polar space and transformed into Cartesian space using

$$\mathbf{z}_k = \begin{bmatrix} r_k \cos(\phi_k) \\ r_k \sin(\phi_k) \end{bmatrix}. \quad (21)$$

Since the polar measurement standard deviation  $\sigma_r$  for range and  $\sigma_\phi$  for the detection angle are small, the associated covariance matrix in Cartesian coordinates is approximated using

$$\mathbf{R}_k \approx \frac{1}{2} \begin{pmatrix} \sigma_r^2 - r_k^2 \sigma_\phi^2 & & \\ & \sin(2\phi_k) & \\ & \sin(2\phi_k) & b - \cos(2\phi_k) \end{pmatrix} \quad (22)$$

$$b = \frac{\sigma_r^2 + r_k^2 \sigma_\phi^2}{\sigma_r^2 - r_k^2 \sigma_\phi^2}.$$

A more detailed discussion of optimal transformation for polar into Cartesian to minimize transformation bias and covariance errors can be found in [27].

For each axis, the nearly constant acceleration (CA) model is used as the linear transition model:

$$\tilde{\mathbf{F}} = \begin{bmatrix} 1 & T & \frac{T^2}{2} \\ 0 & 1 & T \\ 1 & 0 & e^{-T/\tau_{CA}} \end{bmatrix}, \quad \tilde{\mathbf{Q}} = \begin{bmatrix} 0 & 0 & 0 \\ 0 & 0 & 0 \\ 0 & 0 & \sigma_v^2(1 - e^{-2T/\tau_{CA}}) \end{bmatrix}$$

Hence, the two-dimensional system reads  $\mathbf{F} = \tilde{\mathbf{F}} \otimes \mathbf{I}_2$  and  $\mathbf{Q} = \tilde{\mathbf{Q}} \otimes \mathbf{I}_2$ . The parameters for the model are given in Table IV.

For the second filter (Filter B), the polar measurements including range rate are incorporated for the update step using the sensor model in (8). Therefore, the unscented Kalman filter (UKF) is adopted. As motion model, the Constant Turn Rate and Velocity Model are used with transition function and process noise as follows:

$$f(\mathbf{x}_k) = \begin{pmatrix} x + T \frac{V(\sin(\psi + \omega T) - \sin\psi)}{\omega} \\ y + T \frac{V(\cos(\psi + \omega T) - \cos\psi)}{\omega} \\ \psi + T\omega \\ V \\ \omega \end{pmatrix}, \mathbf{Q}_\omega = \begin{bmatrix} 0 & 0 & 0 & 0 & 0 \\ 0 & 0 & 0 & 0 & 0 \\ 0 & 0 & \frac{T^3 \sigma_\omega^2}{2} & \frac{T^2 \sigma_\omega^2}{2} & 0 \\ 0 & 0 & \frac{T^2 \sigma_\omega^2}{2} & T \sigma_\omega^2 & 0 \\ 0 & 0 & 0 & 0 & T \sigma_v^2 \end{bmatrix}$$

The parameters for both motion models and extension estimation used in the simulation are given in table IV. The parameters for the extension estimate are the same for both filters. As the GPDA filters do not include target birth, the number of targets in each scenario is assumed to be constant and is known a priori.

### A. Single Target Case

One vessel with size  $8m \times 2m$  is moving on a trajectory as shown in Figure 1. For this data, one GPDA filter using the linear configuration and a second filter using CTRV and Doppler measurements are applied. For each filter, 500 Monte Carlo runs have been executed. The velocity profile for each trajectory is randomly generated with a standard deviation for velocity change of  $\sigma_V = 0.2m/s^2$ . The mean velocity is  $3.5m/s$ . In addition to the GPDA results, the filter errors are shown if the correct data association would be known, e.g. no clutter is present. For both proposed updating schemes, the suggested tracking algorithm provides a stable track. The RMS error for position is shown in Figure 2, and heading and velocity errors are shown in Figure 3. The GPDA results show no significant distance to the estimation results with known associations. Using the range rate measurements with a UKF leads to performance gain in heading and especially velocity estimates. With increasing detection count, the performance gain due to nonlinear filtering will obviously decrease further.

The extension error is computed using  $RMSE_{\mathbf{x}} = \sqrt{\frac{1}{500} \sum_j \text{tr}[(\mathbf{X}_{k|k}^j - \mathbf{X}_k)^2]}$  and is shown in Figure 4. The results for the extension estimates are comparable; however, during the turning maneuvers, the GPDA with UKF has slightly better results. This gain is obviously due to a better clutter rejection, since in the optimal case there is no difference between the two methods. As can be seen in Figure 1, in both cases, no good match is achieved for ellipse orientation and size during the turning maneuvers. An improvement could be achieved using the prediction step, as proposed in [12]. The average errors of all runs over time are given in Table V.

### B. Multi Target Case

To evaluate the joint data association, a scenario with two vessels of the same size as above is considered. The trajectory is chosen in such a way that the vessels meet in the sensor center field of view, move in parallel through a turning maneuver, and then split off again. The distance between the two vessels during the parallel phase is equal to the vessels' width. The distance is chosen in such a way that if two single filters as in the previous part were used, the estimated trajectories would merge. At this point, a track is considered merged if a centroid position is inside another

CA	$\sigma_v = 0.15m/s^2$	$\tau_{CA} = 2s$
CTRV	$\sigma_V = 0.25m/s^2$	$\sigma_\omega = 0.25^\circ/s$
Extension	$c = 1/4$	$\tau = 2s$

TABLE IV  
PROCESS NOISE PARAMETERS FOR SYSTEM MODELS

Model	Position	Heading	Velocity	Length	Width
Linear	0.61 m	$5.3^\circ$	0.45m/s	0.42 m	0.91 m
UKF	0.48 m	$3.7^\circ$	0.21m/s	0.55 m	0.63 m

TABLE V  
RMSE FOR GPDA WITH LINEAR CARTESIAN FILTER AND POLAR FILTER USING UKF FOR 500 MONTO CARLO SIMULATIONS

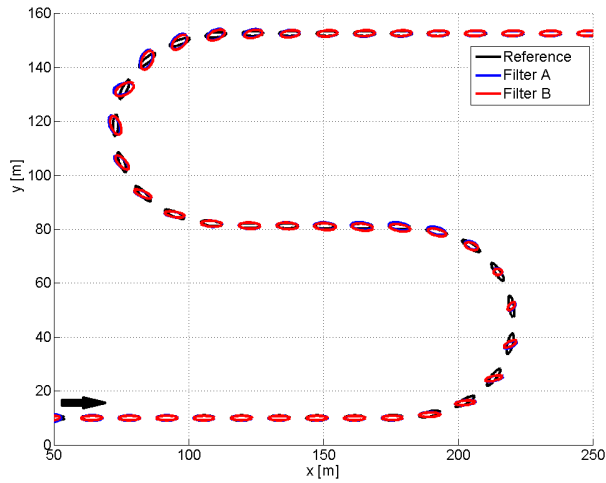


Fig. 1. Path of reference object and estimated position and extension for linear and Doppler-based filtering

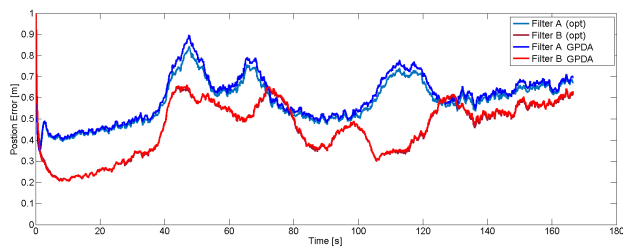


Fig. 2. RMSE horizontal position over time. No significant difference between filtering with known measurement association (opt) and GPDA solution occurs.

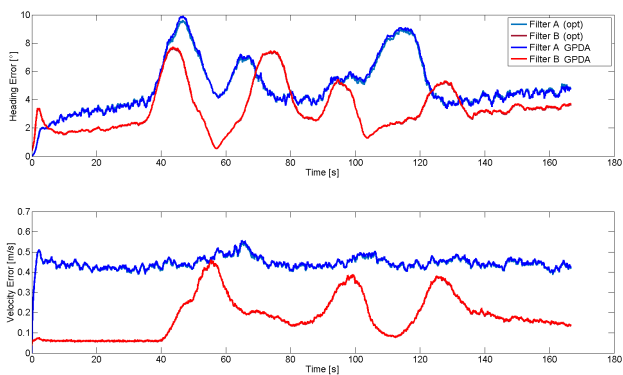


Fig. 3. RMSE of heading and velocity. The results for optimal association and GPDA filtering are practically identical.

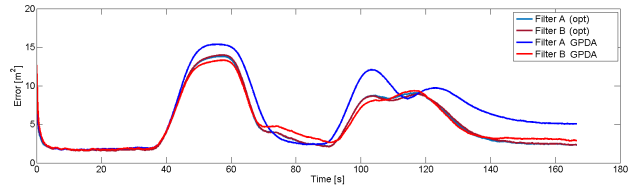


Fig. 4. RMSE of object extension

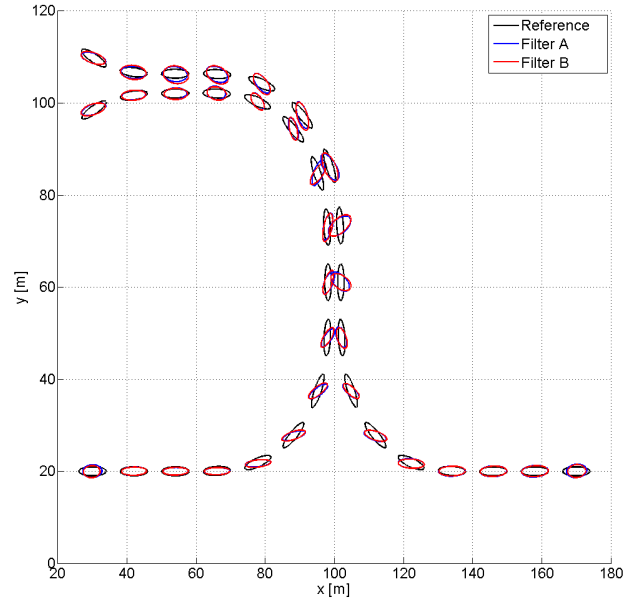


Fig. 5. Path of reference objects (black) and estimated position and extension for linear (blue) and Doppler-based filtering (red)

target's extension ellipse. Again, for this scenario, Filters A and B are used with the same parameters for dynamics and sensor model, and 500 Monte Carlo simulations have been executed. Over all runs, the estimated trajectories of both vessels remain separated all the time when using the UKF, but merged in 70 (14%) runs when using Filter A. All merges occurred during the common turning phase. However, as can be seen from Figure 5, an overlapping of the extension ellipses is still possible for the UKF as well. The kinematic estimation results for the stable tracks are similar to the performance of the single target case and thus not shown in this paper due to space considerations.

## VI. EXPERIMENTAL RESULTS

The presented tracking algorithms have been applied to the following system: An automotive radar system was mounted on a small vessel (Figure 6). The radar has an opening angle of  $\pm 26^\circ$  for a 60m short range mode. In the test scenario, the host vessel is following a target vessel in a varying distance. The driven trajectory is shown in Figure 7. In addition to the turning maneuver, this trajectory contains two times the passage of a bridge. This leads to a significant increase in

the received measurement count in that region. The tracking is done in body-fixed coordinates of the host vehicle. Thus, before each update step, the motion of the host vehicle has to be compensated for in the target state and extension estimate. This is done using the velocity measurement from a GPS and the yaw rate from an automotive gyro. The measurement filtering is done with a CTRV model for the ego motion. For the extension ellipse, only the heading change is used to rotate  $\mathbf{X}_k$ . The remaining parameters are identical to those used for the simulation process. Since only a single target ship is available for the experiments, only the results for GPDA are shown here.

The results of the position and estimated extension ellipses are shown in Figure 7. As can be seen, there is a significant deviation in reference position, received measurements, and track estimate before the first passage of the bridge. The accuracy of the proposed system is evaluated based on the recorded GPS traces for both ships. While the kinematic state of the host vessel was measured using a differential RTK GPS with two antennas, for the target vessel only a low-cost GPS receiver was available. This already leads to relative positional uncertainty of a few meters. Moreover, it should be noted that both GPS systems lose the satellite beneath the bridge, which is why only model-based estimations are available in these cases. Consequently, it is practically impossible to calculate a real ground truth of the relative position of the target to the host. Thus, the shown traces and the corresponding calculated RMS errors for tracked to measured states can only show trends. Tests with two DGPS systems are on schedule.

Model	Position	Heading	Velocity	Length	Width
Linear	1.98 m	6.7°	0.13m/s	0.92 m	1.11 m
UKF	1.92 m	5.5°	0.07m/s	0.60 m	0.90 m

TABLE VI  
RMSE BETWEEN ESTIMATED AND GPS MEASURED STATES

The estimated heading and velocity are shown in Figure 8. Since the target vessel is moving with constant velocity, the gain when using range rates is low here. However, as expected, the highest impact of the Doppler speed is achieved in the data association process. This can be seen from Figure 9 where the target's extent is plotted. For better readability, here the length, width, and orientation of the estimated ellipse as well as true



Fig. 6. Vessels for sea test: The radar is mounted above the front window of the host, approximately 1.5 m above the water surface. The target size is 8.2 m. in length and 2.5 m. in width

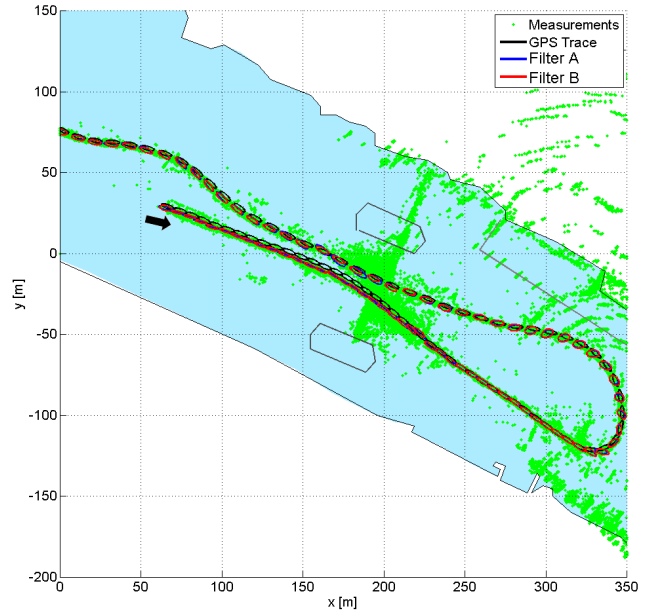


Fig. 7. Path of reference object, with one turn and two bridge crossings. The extension ellipses are plotted at an interval of 4s.

values are shown. When the target is passing through the bridge (e.g. at time 250s), the number of associated measurements for Filter A increases, thus leading to an overestimation of the target size. This is not the case for Filter B, where the target measurements are more clearly distinct from static object measurements. Thus, there is a better estimation of the extension for the real data process.

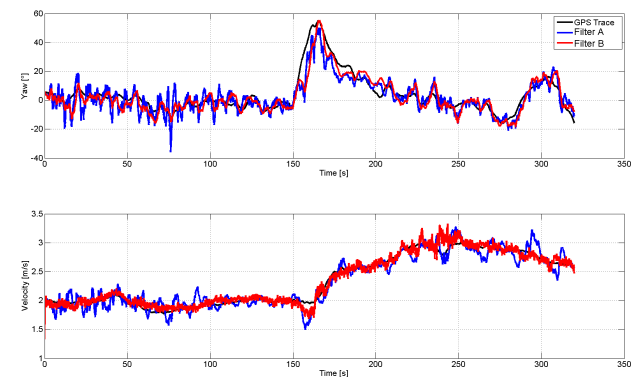


Fig. 8. Estimated heading and velocity over Time

## VII. CONCLUSION

In this paper, the problem of tracking surface vessels on inland waterways using automotive radar sensor is considered. Hence, the concept of random matrices to estimate kinematic state and target extension in parallel is used. To solve the data association problem, the GPDA and GJPDA filters are applied. Based on the assumption that the expected number

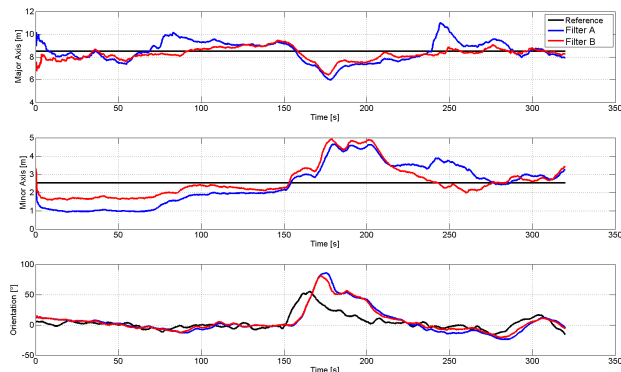


Fig. 9. Estimates size and ellipse orientation of the target vessel over time

of detections from targets is Poisson-distributed and known in the mean, it was shown that this procedure can reliably track an object under clutter. In addition, the influence of using the Doppler measurement was evaluated as well. It was shown that this can improve target state estimate and certainly improves the data association. Since the GPDA is a single-target tracker, for the multi-target case, the GJPDA is considered and it was shown that it can separate close objects properly. However, due to the combinatorial problem, it can only be used if the count for tracks and measurements in the association cluster is small. To solve this, heuristic search schemes are currently investigated in order to use only the  $m$ -best association hypothesis. In future research, the GPDA will also have to be extended to handle an unknown expected number of detections per target.

#### REFERENCES

- [1] K. Granstrom, C. Lundquist, and U. Orguner, "A gaussian mixture phd filter for extended target tracking," in *Information Fusion (FUSION), 2010 13th Conference on*, July 2010, pp. 1–8.
- [2] M. J. Waxman and O. E. Drummond, "A bibliography of cluster (group) tracking," *Proc. SPIE*, vol. 5428, pp. 551–560, 2004. [Online]. Available: <http://dx.doi.org/10.1117/12.548357>
- [3] L. Mihaylova, A. Y. Carmi, F. Septier, A. Gning, S. K. Pang, and S. Godsill, "Overview of bayesian sequential monte carlo methods for group and extended object tracking," *Digital Signal Processing*, vol. 25, no. 0, pp. 1 – 16, 2014.
- [4] M. Buhren and B. Yang, "Simulation of automotive radar target lists using a novel approach of object representation," in *Intelligent Vehicles Symposium, 2006 IEEE*, 2006, pp. 314–319.
- [5] L. Hammarstrand, L. Svensson, F. Sandblom, and J. Sorstedt, "Extended object tracking using a radar resolution model," *Aerospace and Electronic Systems, IEEE Transactions on*, vol. 48, no. 3, pp. 2371–2386, 2012.
- [6] C. Lundquist, K. Granstrom, and U. Orguner, "Estimating the shape of targets with a phd filter," in *Information Fusion (FUSION), 2011 Proceedings of the 14th International Conference on*, July 2011, pp. 1–8.
- [7] K. Granstrom, C. Lundquist, and O. Orguner, "Extended target tracking using a gaussian-mixture phd filter," *Aerospace and Electronic Systems, IEEE Transactions on*, vol. 48, no. 4, pp. 3268–3286, October 2012.

- [8] J. Koch, "Bayesian approach to extended object and cluster tracking using random matrices," *Aerospace and Electronic Systems, IEEE Transactions on*, vol. 44, no. 3, pp. 1042–1059, 2008.
- [9] M. Baum and U. Hanebeck, "Random hypersurface models for extended object tracking," in *Signal Processing and Information Technology (ISSPIT), 2009 IEEE International Symposium on*, Dec 2009, pp. 178–183.
- [10] M. Feldmann, D. Franken, and W. Koch, "Tracking of extended objects and group targets using random matrices," *Signal Processing, IEEE Transactions on*, vol. 59, no. 4, pp. 1409–1420, April 2011.
- [11] U. Orguner, "A variational measurement update for extended target tracking with random matrices," *Signal Processing, IEEE Transactions on*, vol. 60, no. 7, pp. 3827–3834, July 2012.
- [12] J. Lan and X. Li, "Tracking of extended object or target group using random matrix - part i: New model and approach," in *Information Fusion (FUSION), 2012 15th International Conference on*, July 2012, pp. 2177–2184.
- [13] —, "Tracking of extended object or target group using random matrix - part ii: Irregular object," in *Information Fusion (FUSION), 2012 15th International Conference on*, July 2012, pp. 2185–2192.
- [14] M. Wieneke and W. Koch, "A pmht approach for extended objects and object groups," *Aerospace and Electronic Systems, IEEE Transactions on*, vol. 48, no. 3, pp. 2349–2370, JULY 2012.
- [15] M. Wieneke and S. Davey, "Histogram-pmht for extended targets and target groups in images," *Aerospace and Electronic Systems, IEEE Transactions on*, vol. 50, no. 3, pp. 2199–2217, July 2014.
- [16] H. Zhu, T. Ma, S. Chen, and W. Jiang, "A random matrix based method for tracking multiple extended targets," in *Information Fusion (FUSION), 2014 17th International Conference on*, July 2014, pp. 1–8.
- [17] K. Granstrom and U. Orguner, "A phd filter for tracking multiple extended targets using random matrices," *Signal Processing, IEEE Transactions on*, vol. 60, no. 11, pp. 5657–5671, Nov 2012.
- [18] Y. Bar-Shalom, T. Kirubarajan, and X. Lin, "Probabilistic data association techniques for target tracking with applications to sonar, radar and eo sensors," *Aerospace and Electronic Systems Magazine, IEEE*, vol. 20, no. 8, pp. 37–56, 2005.
- [19] B. Habtemariam, R. Tharmarasa, T. Kirubarajan, D. Grimmett, and C. Wakayama, "Multiple detection probabilistic data association filter for multistatic target tracking," in *Information Fusion (FUSION), 2011 Proceedings of the 14th International Conference on*, July 2011, pp. 1–6.
- [20] R. Schubert, C. Adam, E. Richter, S. Bauer, H. Lietz, and G. Wanielik, "Generalized probabilistic data association for vehicle tracking under clutter," in *Intelligent Vehicles Symposium (IV), 2012 IEEE*, 2012, pp. 962–968.
- [21] C. Adam, R. Schubert, and G. Wanielik, "Radar-based extended object tracking under clutter using generalized probabilistic data association," in *Intelligent Transportation Systems - (ITSC), 2013 16th International IEEE Conference on*, Oct 2013, pp. 1408–1415.
- [22] B. Habtemariam, R. Tharmarasa, T. Thayaparan, M. Mallick, and T. Kirubarajan, "A multiple-detection joint probabilistic data association filter," *Selected Topics in Signal Processing, IEEE Journal of*, vol. 7, no. 3, pp. 461–471, June 2013.
- [23] S. Julier and J. Uhlmann, "Unscented Filtering and Nonlinear Estimation," *Proceedings of the IEEE*, vol. 92, no. 3, pp. 401–422, Mar. 2004.
- [24] J. Gertz, "Multisensor Surveillance for Improved Aircraft Tracking," *Lincoln Laboratory Journal*, vol. 2, pp. 381–396, 1989.
- [25] K. Granstrom and U. Orguner, "New prediction for extended targets with random matrices," *Aerospace and Electronic Systems, IEEE Transactions on*, vol. 50, no. 2, pp. 1577–1589, April 2014.
- [26] R. Schubert, E. Richter, and G. Wanielik, "Comparison and evaluation of advanced motion models for vehicle tracking," in *Information Fusion, 2008 11th International Conference on*, June 2008, pp. 1–6.
- [27] D. Franken, "Consistent unbiased linear filtering with polar measurements," in *Information Fusion, 2007 10th International Conference on*, July 2007, pp. 1–8.